ACADEMIC PRESS

Available online at www.sciencedirect.com

SCIENCE DIRECT®

Experimental Neurology 184 (2003) 196–213

Experimental Neurology

www.elsevier.com/locate/yexnr

Suppression of hippocampal neurogenesis is associated with developmental stage, number of perinatal seizure episodes, and glucocorticosteroid level☆

H. Liu,[a] J. Kaur,[a] K. Dashtipour,[b] R. Kinyamu,[b] C.E. Ribak,[b] and L.K. Friedman[a,*]

[a] *New Jersey Neuroscience Institute, Seton Hall University, South Orange, NJ 07079, USA*

[b] *Department of Anatomy and Neurobiology, University of California, College of Medicine, Irvine, CA 92697, USA*

Received 29 July 2002; revised 27 January 2003; accepted 26 March 2003

Abstract

Seizures increase dentate granule cell proliferation in adult rats but decrease proliferation in young pups. The particular period and number of perinatal seizures required to cause newborn granule cell suppression in development are unknown. Therefore, we examined cell proliferation with bromodeoxyuridine (BrdU) immunohistochemistry during the peak of neurogenesis (e.g., P6 and P9) and at later postnatal ages (e.g., P13, P20, or P30) following single and multiple episodes of perinatal status epilepticus induced by kainate (KA). Because an inverse relationship exists between glucocorticosteroids (CORT) levels and granule cell proliferation, plasma CORT levels and electroencephalographic (EEG) activity were simultaneously monitored to elucidate underlying mechanisms that inhibit cell proliferation. In control animals, the number of BrdU-labeled cells increased then declined with maturation. After 1× KA or 2× KA administered on P6 and P9, the numbers of BrdU-labeled cells were not different from age-matched controls. However, rat pups with 3× KA (on P6, P9, and P13) had marked suppression of BrdU-labeled cells 48–72 h after the last seizure (43 ± 6.5% of control). Cell proliferation was also significantly inhibited on P20 after 2× KA (to 56 ± 6.9%) or 3× KA (to 54 ± 7.9%) and on P30 with 3× KA (to 74.5 ± 8.2% of age-matched controls). Cell death was not apparent as chromatin stains showed increased basophilia of only inner cells lining the granule cell layers, in the absence of eosinophilia, argyrophilia, or terminal deoxynucleotidyl dUTP nick endlabeling (TUNEL) labeling at times examined. In P13 pups with 3× KA, electron microscopy revealed an increased number of immature granule cells and putative stem cells with irregular shape, condensed cytoplasm, and electron dense nuclei, and they were also BrdU positive. The EEG showed no relationship between neurogenesis and duration of high-synchronous ictal activity. However, endocrine studies showed a correlation with BrdU number and age, sustained increases in circulating CORT levels following 1× KA on P6 (0.7 ± 0.1 to 2.40 ± 0.86 μg/dl), and cumulative increases that exceeded 10 μg/dl at 4–8 h after 3× KA on P13 or P20. In conclusion, a history of only one or two perinatal seizure(s) can suppress neurogenesis if a second or third seizure recurs after a critical developmental period associated with a marked surge in CORT. During the first 2 weeks of postnatal life sustained increases in postictal circulating CORT levels but not duration or intensity of ictal activity has long-term consequences on neurogenesis. The occurrence of an increased proportion of immature granule cells and putative stem cells with irregular morphology in the absence of neurodegeneration suggests that progenitors may not differentiate properly and remain in an immature state.

Keywords: Newly born; Perinatal; Inhibition; Multiple seizures; Dentate gyrus

Introduction

Ongoing neurogenesis occurs within discrete regions of the brain throughout development and adulthood. The dentate granule cell layer of the hippocampus was previously characterized as a region of continuous but age-dependent proliferation in the rodent (Altman and Das, 1965; Kuhn et al., 1996), monkey (Kornack and Rakic, 1999; Nowakowski and Rakic, 1981; Rakic, 1985), and human (Eriksson et al., 1998). Bromodeoxyuridine (BrdU) and [^{3}H]thymidine DNA labeling studies demonstrated that granule cell progenitors are numerous during the first postnatal week in rats, a time when adrenal steroid levels are low (Bayer, 1980; Gould and Tanapat, 1999). Autoradiography showed that the majority of cells undergo their last phase of DNA synthesis between the 5th and 7th postnatal days (Schless-

☆ This study was presented in abstract form as "Multiple seizures suppress neurogenesis in the developing dentate gyrus" at the 2nd International European Society for Neuroscience meeting held in Brighton, England, 2000.

* Corresponding author. Department of Neuroscience, Seton Hall University/JFK Medical Center, 400 S Orange Avenue, South Orange, NJ 07079, USA. Fax: +1-973-275-2370.

E-mail address: friedmli@shu.edu (L.K. Friedman).

0014-4886/03/$ – see front matter © 2003 Elsevier Science (USA). All rights reserved.
doi:10.1016/S0014-4886(03)00207-3

inger et al., 1975). From the second postnatal week to adulthood, proliferation declines (Sapolsky and Meaney, 1986). Corticosterone levels and *N*-methyl-D-aspartate (NMDA) receptor activation appear to regulate the rate of this proliferation (Gould and Tanapat, 1999). For example, during this period, loss of glucocorticosteroids (CORT) by adrenalectomy results in selective granule cell degeneration of the dentate gyrus (Sloviter et al., 1989, 1993). Pharmacological antagonists of NMDA receptors (e.g., MK801) increase granule cell death, CORT suppresses cell division (Gould et al., 1992, 1994), and NMDA stimulates or supports neurogenesis (Gould and Tanapat, 1997; Tanapat and Gould, 1998). Similarly, in adult animals, increased corticosterone levels or NMDA application highly suppress death of granule cell precursors that may be modulated by an NMDA receptor-mediated pathway (Gould et al., 1997b).

CORT binds to cytoplasmic proteins, and subsequently to specific palindromic DNA sequences called glucocorticosteroid-responsive elements (Beato et al., 1989). Two types of CORT receptors have been characterized in the brain including type I, the kidney mineralocorticoid receptor that has high affinity for corticosterone/cortisol (Kawata et al., 1998). Type II, or glucocorticoid receptors, have low affinity for corticosterone/cortisol and high affinity for dexamethasone (Clayton et al., 1977; Kawata et al., 1998). Both glucocorticoid receptor subtypes are expressed prominently in the hippocampus (McEwen et al., 1969; Morimoto et al., 1996). Although CORT enters the brain and binds preferentially to mineralocorticoid receptors (De Kloet et al., 1987; Reul and de Kloet, 1985), glucocorticoid receptor binding increases with increased plasma CORT levels triggered by stress (Ratka et al., 1989) or during late nocturnal sleep (Dallman et al., 1989).

In adult rats, numerous pathological conditions enhance neurogenesis. For example, a single episode of status epilepticus induced by pilocarpine (Parent et al., 1997) or kainic acid (Gray and Sundstrom, 1998) increases neurogenesis. Kindling (Parent et al., 1998; Scott et al., 1998), repeated electroconvulsive shock stimulation (ECS) (Scott et al., 2000), ibotenic acid (Gould et al., 1997a), or chronic antidepressant treatment (Malberg et al., 2000) also increases the proliferation of granule cells of the dentate gyrus. Moreover, transient global ischemia increases the proliferation of dentate granule cells, possibly contributing to the survival of this region (Kee et al., 2001). Raised levels of granule cell progenitors are also observed with an enhanced learning environment (Gould et al., 1999a; Kempermann et al., 1997). Therefore, excitatory stimuli associated with increased release of glutamate upregulate the rate of stem cell proliferation.

There is a paucity of data on the effects of perinatal seizures on hippocampal neurogenesis as a function of age. Retrospective studies have shown that daily electroconvulsive seizures induced between P2 and P11, or generalized flurothyl seizures induced in 4-day-old rat pups, irreversibly decrease brain DNA content, cell number, cell size, and total brain weight (Wasterlain and Plum, 1973; Wasterlain, 1976, 1979). Seizure activity induced later in life had no effect on brain weight, size or cell number (Wasterlain and Plum, 1973). Suga and Wasterlain (1980) later showed that a delayed reduction occurs in the number of proliferating cells (labeled by [^{3}H]thymidine) of the cerebellum, if status epilepticus is induced with bicuculline at perinatal ages. More recently, during the course of our study, McCabe et al. (2001) demonstrated that a series of 25 flurothyl seizures induced during the first 5 days of postnatal development result in suppression of granule cell progenitors after 3 or 14 days. This group also reported earlier that repeated flurothyl seizures, induced in the perinatal period, lead to increases in dentate granule cell number in adulthood (Holmes et al., 1998). In contrast, a single systemic injection of methamphetamine administered to immature gerbils reduced granule cell proliferation when measured as adults (Hildebrandt et al., 1999). The present study characterized the minimum number of episodes of perinatal status epilepticus required to suppress neurogenesis. Total circulating CORT levels were also measured as a function of age and seizure history. Suppression of dentate granule cell neurogenesis was correlated with the age of the animal, circulating CORT levels, and the particular history of perinatal seizures but not with paroxysmal activity in the electroencephalogram (EEG).

Materials and methods

Kainate injections

Sprague-Dawley rats of several postnatal (P) ages were used. Animals were given food and water ad libitum and kept on a 12-h light/dark cycle at room temperature (55% humidity) in our own accredited animal facility in accordance with NIH guidelines. To test the effects of single or multiple seizures on neurogenesis, kainate (KA) was administered (once, twice, or three times) as described in Table 1. At the middle age (P13), doses of 4–5 mg/kg of KA, typically used to induce sustained status epilepticus in naîve animals (Albala et al., 1984; Friedman et al., 1997; Nitecka et al., 1984; Sperber et al., 1991), killed the P13 pups with 3× KA (on P6, P9, and P13). Therefore, a lower dose (2.5 mg/kg) was used to induce seizures. Inherent doses of KA typically used to induce status epilepticus were used for the other ages, i.e., P6 (2 mg/kg s.c.), P9 (2 mg/kg s.c.), P20 (7 mg/kg i.p.), and P30 (15 mg/kg i.p.).

Animals were divided into five experimental groups according to the age and number of KA injections received (Table 1). Group I animals were injected with KA once (1× KA) either on P6, P9, P13, P20, or P30 ($n = 4$–11 per age). Group II animals were injected two times with KA (2× KA), once on P6 and again on P9 ($n = 5$), or on P6 and P13

Table 1
Experimental design of Kainate (KA) and bromodeoxyuridine (BrdU) injections and glucocorticosteroid (CORT) measurements[a]

	1 × KA	2 × KA	3 × KA	No. of BrdU Inj.
Group I	P6; P9; P13; P20; P30			2
Group II		P6, P9; P6, P13; P6, P20		3
Group III			P6, P9, P13	4
Group IV			P6, P9, P20	4
Group V			P6, P9, P30	4

[a] Age-matched controls for each experimental group were treated with equal volumes and numbers of phosphate-buffered saline and BrdU injections (inj.). CORT was measured for Groups I–IV.

($n = 4$), or on P6 and P20 ($n = 7$). Group III received three injections of KA (3× KA), one on P6, the second on P9, and the third on P13 ($n = 15$). Group IV was also injected three times, on P6, P9, and P20 ($n = 6$). Finally, Group V also received a total of three injections of KA, on P6, P9, and P30 ($n = 6$). For each experimental group, age-matched control littermates received equivalent volumes of phosphate-buffered saline (PBS; 0.1 M, pH 7.4).

BrdU injections

To label a proportion of mitotically active cells that appear following status epilepticus, BrdU (Zymed, 10 mg/kg) was administered systemically to each group by a modification of Parent et al. (1997). Because BrdU is a thymidine analogue and gets incorporated into DNA only during the DNA-synthetic phase of the cycle (S phase) (del Rio and Soriano, 1989) and BrdU is available for about 30 min (Packard et al., 1973), all groups received BrdU (i.p.) following each seizure and again 4 h before they were killed. Specifically, animals that received one injection of KA had two BrdU injections (Table 1). Animals with two injections of KA had three injections of BrdU, and animals with three injections of KA had four injections of BrdU. Thus, animals with a history of episodes of status epilepticus prior to the end of the second postnatal week (Group III) had four injections (P6, P9, and P13). The older aged experimental animals (Groups IV and V) also had four injections but with a longer time interval before their fourth BrdU treatment (Table 1). To obtain control labeling for each experimental group, age-matched littermates were given the same number of BrdU injections of equal concentration at the same time.

Electroencephalography

A separate group of animals was anesthetized with a mixture of 70 mg/kg ketamine and 6 mg/kg xylazine. Bipolar electrodes (Narishege, Japan) was stereotaxically implanted into the right hippocampus (coordinates in milliliters with respect to Bregma, for P13: AP, −2.7; L, 1.8; D, −2.4; P20: AP, −2.7; L, 1.8; D, −2.6; P30: AP, −2.7; L, 2.0; D, −2.6; incisor bar at −3.5). The electrodes were perpendicular, angled at 0 degrees from the vertical sagittal plane. Pups became active 1–3 h following the surgery and were returned to their lactating mother. For EEG recordings, animals were paired in an insulated chamber and were connected to the recording set up through flexible, low-noise leads that permitted movement (Nowakowski and Rakic, 1981; Oliveras et al., 1990). Composite extracellular signals from the electrodes were routed through a high impedance probe, amplified by X Cell 3 × 4 amplifiers (FHC), and connected through the Data Wave interface to an IBM computer. EEG tracings were analyzed with Data Wave Technologies software. Onset to single spikes and long trains of high-synchronous events were counted and the duration measured in seconds. The 3 × KA rats had KA on P6, P9, and P13 ($n = 8$), or P20 ($n = 10$), or P30 ($n = 5$), and were compared with the 1× KA rat pups on P13 ($n = 12$), P20 ($n = 10$), or P30 ($n = 5$). Saline-injected, age-matched control rats were also used for comparison ($n = 7$).

Radioimmunoassay

To determine whether total plasma CORT levels correspond with suppression of neurogenesis and spike activity, blood was collected from a separate group of P6–P30 ages at several time points (0.5, 0.75, 1, 2, 4, 8, 24, 48, or 72 h) and after 1×, 2×, or 3× KA administrations. Baselines were measured from age-matched controls. Stock solutions of corticosterone were prepared (1 μg/ml) in absolute ethanol to obtain standard solutions (15, 31, 62, 125, 250, 500, and 1000 pg/0.1 ml). After centrifugation, diluted serum (0.1 ml) from each control and experimental group was added in polypropylene tubes with 0.5 ml of diluted antiserum (anti-corticosterone or anti-hydrocortisone, Sigma). Tubes were vortex mixed and then incubated for 30 min at room temperature. Diluted tritiated radioactive tracer was added and incubated for 1 h at 37°C. Tubes were cooled down and cold dextran-coated charcoal suspension was added. Tubes were vortex mixed and incubated for 10 min at 0°C ice water. After centrifugation at 2000 × g for 15 min at 4°C, supernatant was removed from each tube, and scintillation cocktail added to determine the amount of radioactivity present. The concentrations of plasma CORT were calculated and compared with the standard curve.

Immunohistochemistry

Animals were anesthetized with pentobarbital (10–20 mg/kg i.p.). Transcardiac perfusion with saline was carried out to clear the blood followed by 4% paraformaldehyde (PFA)/PBS, to initiate fixation. Immunohistochemistry was performed on coronal vibratome sections (40 μm) through the septotemporal extent of the hippocampus. For BrdU immunostaining, sections were submerged in quenching solution (3% H_2O_2 in absolute methanol) for 10 min, then rinsed with PBS. Sections were incubated in 0.125% trypsin at 37°C for 3–10 min for digestion, rinsed in distilled water, and denatured by 3 N HCl for 20 min. Sections were incubated in 0.3% bovine serum albumin for 10 min, incubated in biotinylated mouse anti-BrdU (Zymed) for 1 h at 23°C, then incubated in streptavidin-peroxidase (Zymed) for 10 min at room temperature. The reaction product was detected by using 3,3-diaminobenzidine tetrahydrochloride mixture (DAB; 0.5 mg/ml). For terminal deoxynucleotidyl dUTP nick endlabeling (TUNEL) immunostaining a commercially available labeling kit was used (Oncogene). Sections were incubated with proteinase K (0.02 mg/ml in 10 mM Tris, pH 8) for 20 min at 23°C, followed by incubation with 3% H_2O_2 to inactivate endogenous peroxidases, and rinsed with TBS (Tris-buffered saline, pH 7.6), transferase, and biotinylated-uridine. The reaction product was visualized with DAB and sections were lightly counterstained with 1% methyl green. Sections were dehydrated in a series of graded ethanols, cleared, and coverslips were applied with Permount.

Double-labeling immunofluorescence

Double-immunolabeling was carried out on Group III experimental rats at 48 h and on age-matched controls (n = 5). For labeling of BrdU (Accurate Scientific) with NeuN, sections were pretreated as above then incubated with monoclonal rat anti-BrdU conjugated to fluorescein isothiocyanate (FITC) at 4°C overnight. Next day, BrdU-labeled sections were rinsed and then incubated with the second antibody, NeuN (mouse anti-NeuN, 1:100, Chemicon) at 4°C overnight. Sections were then reacted with goat anti-mouse Texas Red IgG (1:100, Vector) for 1 h at room temperature. For BrdU/GFAP double-labeling, monoclonal biotin-mouse anti-BrdU (Zymed) was incubated together with polyclonal GFAP (rabbit anti-GFAP, 1:100, Chemicon) overnight followed by goat anti-mouse Texas Red IgG and goat anti-rabbit FITC IgG (1:100, Vector) for 1 h at room temperature and after thorough removal of primary antibodies. Sections were washed and wet mounted, then dried in the dark. Fluorescent mounting media was applied prior to placing coverslips onto the slides. For visualization and photography, specimens were viewed with a Nikon Eclipse 800 (Micron Optics) immunofluorescence photomicroscope equipped with selective excitation/emission filters for FITC and Texas Red.

BrdU cell counts

Quantification of stereological methods was carried out as described (Gundersen et al., 1988). The dentate gyrus was subdivided into superior blade, inferior blade, and hilus regions (see Fig. 2C). The molecular layer of the lower blade was quantified simultaneously from the same sections. Animals that were killed 48–72 h after the last seizure and multiple BrdU injections had dense, easily delineated nuclear BrdU staining for microscope and computer-assisted analysis. For DAB single-labeled BrdU-positive cells, volumes were quantified from averaged sums from each area of the DG (0.18 mm^2). To avoid overlap of cell counts, the number of BrdU-labeled cells was measured from four coronal sections and averaged from three dorsal hippocampal levels [every fifth section between −3.6 and −4.2 mm from Bregma (Paxinos and Watson, 1986)]. Both dark and light stained nuclei were counted manually by using a grid reticule and a 10× lens under phase-contrast microscopy by a blinded examiner. The sections were subsequently scanned with a Nikon Eclipse 800 microscope that was connected to a digital spot camera and to a G3 Macintosh computer. Scanned sections with BrdU-labeled cells were again counted manually by two investigators naive to the experimental condition to assure accuracy. The numbers counted under the two conditions were then averaged. Double-labeled cells were identified with Photoshop 5.0 software after scanning the dentate/hilus at two wavelengths and superimposing the images. Cells colabeled with BrdU and NeuN or BrdU with GFAP were counted in control and experimental brain sections manually with NIH Image software or with Pro Image Plus software (Media Cybergenics, Silver Spring, MD) by two naîve examiners. Immunofluorecent nuclei or star-like shaped astrocytes were counted from four sections per level per rat. To estimate the percentage of BrdU-labeled cells that were neurons, BrdU and NeuN colabeled cells were divided by the total number of BrdU-labeled cells counted and averaged from the hippocampal levels. To estimate the percentage of BrdU-labeled cells that were glia, BrdU and GFAP colabeled cells were divided by the total number of BrdU-labeled cells counted.

Histology

Hematoxylin/eosin and thionin staining were carried out on adjacent air-dried sections from all brains processed for immunohistochemistry and electron microscopy to monitor eosinophilia and/or cell loss. At least four slides with three to four sections per slide were prepared from PBS controls and 3 × KA animals (n = 6) from three hippocampal levels. Brain regions were identified from Nissl-stained sections and the atlas of Paxinos and Watson (1986). Dark blue granule cells of the inner granule cell layer were counted manually with NIH Image software from four sections at three levels per animal after scanning them into a G3

Macintosh computer with a color digital spot camera. The thickness (in centimeters) of the inner layer lining the border of the dentate gyrus was also measured with Adobe Photoshop 5.0 software in control and experimental animals.

Silver impregnation

Degenerating argyrophilic neurons were monitored throughout the hippocampus by the silver impregnation procedure as described previously (Gallyas et al., 1980). Briefly, vibratome sections (40 μm) were washed in distilled water (3 $\times$ 5 min each) and then pretreated with 2% NaOH and 2.5% NH_4OH. Sections were then incubated with silver impregnation solution (0.8% NaOH, 2.5% NH_4OH, and 0.5% $AgNO_3$) for 10 min. After washing, sections were developed in a silicotungstate developer until sections turned golden brown. Sections were mounted onto slides, then washed in 0.5% acetic acid, dehydrated in graded ethanols, coverslipped, and examined under the microscope.

Electron microscopy

Anesthetized rats were perfused transcardially with cold 0.9% saline followed by cold 1.5% glutaraldehyde and 4% paraformaldehyde in 0.1 M PBS buffer (pH 7.4). After perfusion the brain was removed and fixation continued at 4°C overnight. Following fixation, 100-μm sections were cut on a vibratome. The sections were thoroughly washed in phosphate buffer and then placed in 1% osmium tetroxide for 60 min. Sections were then processed for embedding in plastic using a routine protocol that involved dehydration through a series of ethanols and immersion in propylene oxide as described previously (Seress and Ribak, 1990). A flat-embedding procedure was used to facilitate the examination of each section with a light microscope (Leitz). After identifying the hilus, granule cell, and molecular layers, the sections were then trimmed using a single-edged razor blade and a dissecting microscope (Nikon). Ultrathin sections containing the dentate gyrus were cut with an ultramicrotome (Reichert-Jung) and collected on formvar-coated slot grids. Prior to placing the grids in the microscope, the sections were stained with uranyl acetate and lead citrate to enhance contrast. Ultrathin sections were examined with a Philips CM-10 transmission electron microscope.

BrdU electron microscopy

Using the same method of immunohistochemistry, BrdU-labeled cells were visualized by DAB and then sections were treated with 1% osmium tetroxide for 60 min. Thereafter, sections were processed for embedding in plastic following the same dehydration through a series of ethanols and immersion in propylene oxide as explained above.

Electron microscopic analysis

Granule cells extending through the granule cell layer and to the hilar border were counted from Group III rats and from age-matched PBS controls from at least four grids at random with an electron microscope (EM). Each type was identified based on morphology and characterized as mature, immature, and putative stem cells. Mature cells had a regular, round shape and contained cytoplasmic organelles. Immature granule cells were smaller, oval in shape with a watery cytoplasm, lacking organelles. Putative stem cells were similar to the immature granule cells but much smaller in size. The three types were counted from every fifth section five to 10 sections from each control and experimental group to avoid counting cells twice.

Statistical analysis

Significant differences between control and experimental groups for the BrdU-labeling studies were determined by one-way, two-way, and three-way analyses of variance (ANOVAs) followed by the stringent Tukey test for all pairwise and multiple comparisons. The Pearson product moment correlation coefficient (r) was also calculated for comparing numbers of BrdU-labeled cells across the ages with endogenous CORT levels and after 3 $\times$ KA. Significance was set at $P < 0.05$.

Results

Behavioral features as a function of age and seizure history

At the younger ages (P6 or P9), 2 mg/kg KA induced status epilepticus in approximately 90% of the animals within 20–30 min after injection, similar to other reports (Albala et al., 1984; Friedman et al., 1997; Holmes et al., 1988; Nitecka et al., 1984). Behavioral manifestations included scratching, hyperactivity, rotatory locomotion, arrested posture with ataxia, and long bouts of laying on one side with full body tonus. A small percentage of animals (10–13%) died within 2 h of the injection. At P13 with 3 $\times$ KA, a 2.5 mg/kg dose induced status epilepticus in 8 of 15 of the animals (53.3%). Moderate seizures were observed in 6 animals. Only 1 of 15 (6.7%) had mild or no behavioral symptoms. In contrast, naîve P13 pups with 1 $\times$ KA at 2.5 mg/kg had mild or no symptoms (72%). Only 1 of 11 rat pups at P13 exhibited status epilepticus, 18% had moderate seizure behavior, and 2.2% animals died. Automatisms such as scratching and body tonus without loss of postural control were most commonly observed in the animals that exhibited seizure behavior. At the older ages (P20 or P30), manifestations of status epilepticus occurred in most rats and included continuous head nods, rearing with forelimb clonus, and running and jumping as previously described

Table 2
Perinatal seizures (on P6 and P9) produce opposite effects on high-burst synchronous events with maturation[a]

Treatment	Spike onset (min)	Number of burst events	Average duration of burst events (s)	*N*
P13				
1 × KA	29.3 ± 2.5	2.0 ± 0.85	47 ± 15.8	3
3 × KA	25.7 ± 4.0	4.8 ± 0.65[b]	61.3 ± 9.6[b]	8
P20				
1 × KA	15 ± 3.4	35 ± 5	39 ± 2.8	10
3 × KA	21.6 ± 2.6	19 ± 4.7[b]	22.8 ± 8.6[b]	8
P30				
1 × KA	16.2 ± 3.4	23 ± 7	108.3 ± 25	5
3 × KA	19.4 ± 4.2	17.2 ± 7.5	30.8 ± 6.1[b]	5

[a] Values expressed represent the mean ± SEM of spike latency, the number of high-burst synchronous episodes in the electroencephalogram, and their duration with 1 × or 3 × Kainate (KA) at three postnatal ages. The first two injections of KA were administered on P6 and P9, and the third seizure was induced on P13, P20, or P30.

[b] $P < 0.05$, unpaired two-tailed *t* test.

(Albala et al., 1984; Holmes et al., 1988; Nickel and Szelenyi, 1989). Behavioral onset to seizures for the three older ages (Groups III, IV, and V) receiving the third injection of KA (on P13, P20, or P30) was unchanged by a history of perinatal seizures induced on P6 and P9. Thus, seizure behavior was not altered by previous episodes of KA-induced status epilepticus with the exception that the P13 age group with 3 × KA required lower doses of KA to induce the classical symptoms.

EEG activity shows age-dependent effects

The EEG recordings showed age-dependent effects in animals with and without a history of perinatal seizures that were unrelated to the BrdU-labeled cell counts. For example, after 1 × KA on P13, onset of spike and burst activity in the EEG appeared at a similar time as the behavioral manifestations (Table 2). In contrast, the onset of seizure behavior was delayed in P20 rats with 3 × KA. The appearance of long high-synchronous high-frequency burst events in the EEG was significantly increased in Group III P13 pups that had previous KA injections on P6 and P9. Despite that the onset to single spikes was similar at P13 with 3 × KA relative to 1 × KA age-matched controls, the number of spikes with high synchrony significantly increased (Table 2). Eight of 8 pups had high-frequency burst activity of long duration, whereas only 3 of 12 age-matched 1 × KA pups showed high-synchronous events and they were of shorter duration (Table 2). In contrast, Group IV (P20) animals with 3 × KA showed significant reductions in the number and average duration of synchronous high-frequency burst events, but onset to single spikes was unchanged compared to P20 rats with 1 × KA (Table 2). At P30, typical seizure behaviors were also delayed relative to changes in the EEG and compared to onset of seizure behavior in the younger age groups. Although 3 weeks passed before Group V (P30) rats received their last KA injection, the duration of high-burst activity was also significantly shorter after this delay (Table 2). Resistance to seizures after several exposures to KA is consistent with other reports when serial seizures were first initiated at a later age, P20 (Sarkisian et al., 1997).

BrdU labeling to detect changes in neurogenesis

To capture seizure-induced changes in dentate gyrus cell proliferation, BrdU was injected after each seizure and before death as indicated in Table 1. BrdU immunohistochemistry was carried out at 48 or 72 h after the last seizure for each experimental and age-matched control group (see Table 1). In control animals, single-labeling showed age-dependent BrdU-positive patterns. At P6, BrdU-labeled cells were small in size, evenly labeled, highly abundant, and randomly dispersed throughout the hilus and dorsal and ventral blades of the dentate gyrus (Fig. 1A). Many BrdU-positive-labeled cells were also located in the hippocampal layers outside of the dentate gyrus. At P9, the number of BrdU-labeled cells increased, but they were still unorganized and widely dispersed throughout the dentate gyrus (Fig. 1B). At P13, BrdU-labeled cells were well organized; the majority had migrated to the hilar border of the granule cell layer (Fig. 1C). At P20, BrdU-labeled cells not only migrated deeper into the granule cell layer, but also matured into cells with distinct morphological features (Fig. 1H). These were located in all fields of the dentate gyrus. Some BrdU-labeled cells had heterochromatin label that appeared as small spherical deposits of BrdU-positive material without an apparent nuclear membrane, but others had complete nuclear labeling. Heterochromatin staining with this pattern was not found in the central hilus but appeared near the granule cell borders or within the molecular layer, as reported in adult rats (Gould et al., 1997a) and primates (Gould et al., 1996b) and may be due to increased cellular divisions.

BrdU-labeled cells were counted in the dentate gyrus for each group and compared with age-matched controls with

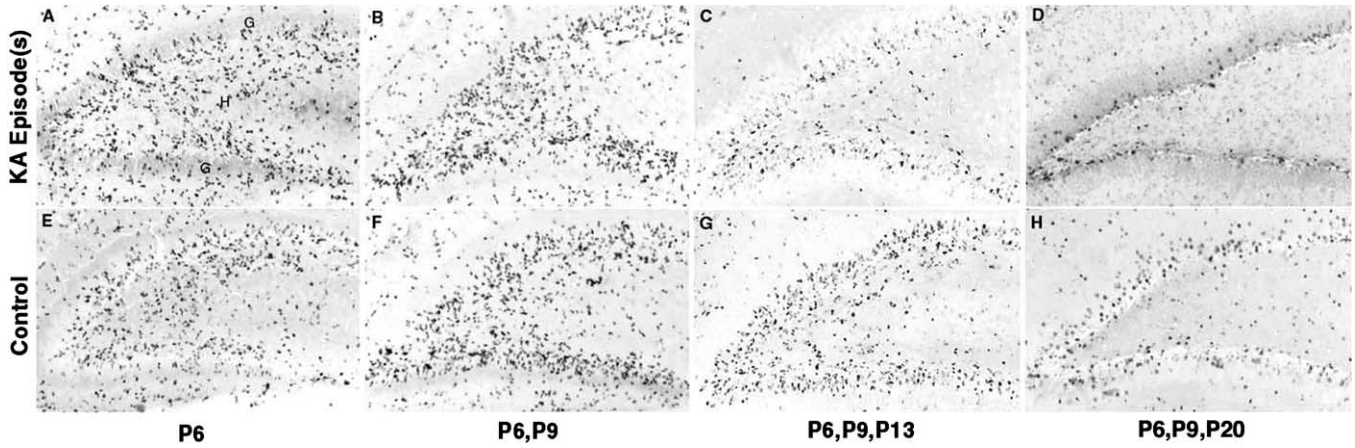

Fig. 1. Photomicrographs of bromodeoxyuridine (BrdU) immunohistochemistry shown as a function of age and number of perinatal seizures at 48 h after the last injection of Kainate (KA). Control BrdU-labeled cells are represented in bottom panels at P6 (E), P9 (F), P13 (G), and P20 (H). Top rows show suppression of cell proliferation by a series of three injections of KA during and after the second postnatal week: (A) 1 × KA on P6; (B) 2 × KA on P6 and P9 (C) 3 × KA on P6, P9, and P13, and (D) 3 × KA on P6, P9, and P20.

the same number of BrdU injections. The highest number of BrdU-labeled cells was found in the P9 control animals with three injections of BrdU (Control baseline: P6, 435 ± 48, $n = 4$; P9, 871 ± 146, $n = 4$; P13, 437 ± 82, $n = 15$) (Figs. 1 and 2A). Statistical analysis confirmed significant differences in the mean values of BrdU-labeled cells among the different ages in the absence of seizures ($F = 29.6$, $P < 0.001$). After 1 × KA and 48 h after injection, the number of BrdU-labeled cells of the dentate granule cell layers was unchanged relative to age-matched controls with equivalent BrdU injections at the ages examined (P6–P30) (Fig. 2A). Group II pups of postnatal week 1 or 2 (i.e., 2 × KA on P6 and P9 or on P6 and P13) also had control levels of BrdU-labeled cells (PBS: 460 ± 62 vs. 2 × KA on P6, P9: 447 ± 60, $n = 4$). In contrast, the total number of BrdU-labeled cells in the hilus and inner granule cell layers was highly suppressed to 43 ± 6.5% in Group III pups with 3 × KA on P6, P9, and P13 (188 ± 25, $n = 15$, one-way ANOVA, $P < 0.001$) (Figs. 1 and 2B). The suppression was specific to the inner granule cell layers and not other regions. For example, steady numbers of BrdU-labeled cells were simultaneously counted from the lower blade molecular layers (inner and outer) (P13, 1 × KA: 208 ± 36 vs. controls: 178 ± 31, $n = 5$, $P > 0.05$ and P6, P9, P13, 3 × KA: 183 ± 31, $n = 6$ vs. BrdU-matched control, 201 ± 40, $n = 5$, $P > 0.05$).

Two-way ANOVA revealed that the mean values of BrdU-labeled cells at the different ages were significantly different after allowing for differences in the number of seizure treatments (0 × KA, 1 × KA, vs. 3 × KA, $F = 66.1$, $P < 0.001$). In addition, the difference in BrdU counts after the different seizure treatments was greater than what would be expected by chance after allowing for the effects of age ($F = 75.1$, $P < 0.001$). There was a significant interaction between age and number of seizures so that the effect of the different ages depended upon how many seizure episodes were induced ($F = 9.35$, $P < 0.001$). Pairwise comparisons using the Tukey stringent test also showed significant differences in the total number of BrdU-labeled cells as a function of age and seizure history. For example, for comparisons within the P13 age group, no KA vs. 3 × KA and 1 × KA vs. 3 × KA had significantly different BrdU count values ($P < 0.001$). Quantitative analysis also showed that if the third seizure was given on P20 (Group IV), a significant reduction in BrdU-labeled cells also was observed in the cell layers where the number of BrdU-labeled cells was decreased to 54 ± 7.9% of controls (Fig. 2B). In this age group, a similar highly significant decrease was observed if the animals had a history of one KA seizure on P6 and the second on P20 (56 ± 6.9%). After 3 × KA on P6, P9, and P30 (Group V), the number of BrdU-labeled cells was still significantly reduced but to a lesser degree than the younger ages (74.5 ± 8.2% of control) (Fig. 2B). Thus, multiple episodes of status epilepticus induced by KA during the peak of neurogenesis showed that the developmental stage and number of seizures are critical for suppression of cell proliferation within the dentate gyrus.

Suppression of cell proliferation is related to location

Quantification of BrdU-labeled cells from the dorsal and ventral molecular layer borders of the dentate gyrus and hilus confirmed that there were both age- and region-specific effects. At P6, before BrdU-labeled cells migrate to the hilar/granule cell borders and are scattered throughout the dentate gyrus and have similar morphology, suppression of neurogenesis was highly significant within the upper and lower blades as well as within the hilus (Figs. 2C-D). The largest reduction was observed in the granule cell layers of the lower blade at all of the postnatal ages studied. However, this decrease reached statistical significance only in the younger age group with a history of three perinatal

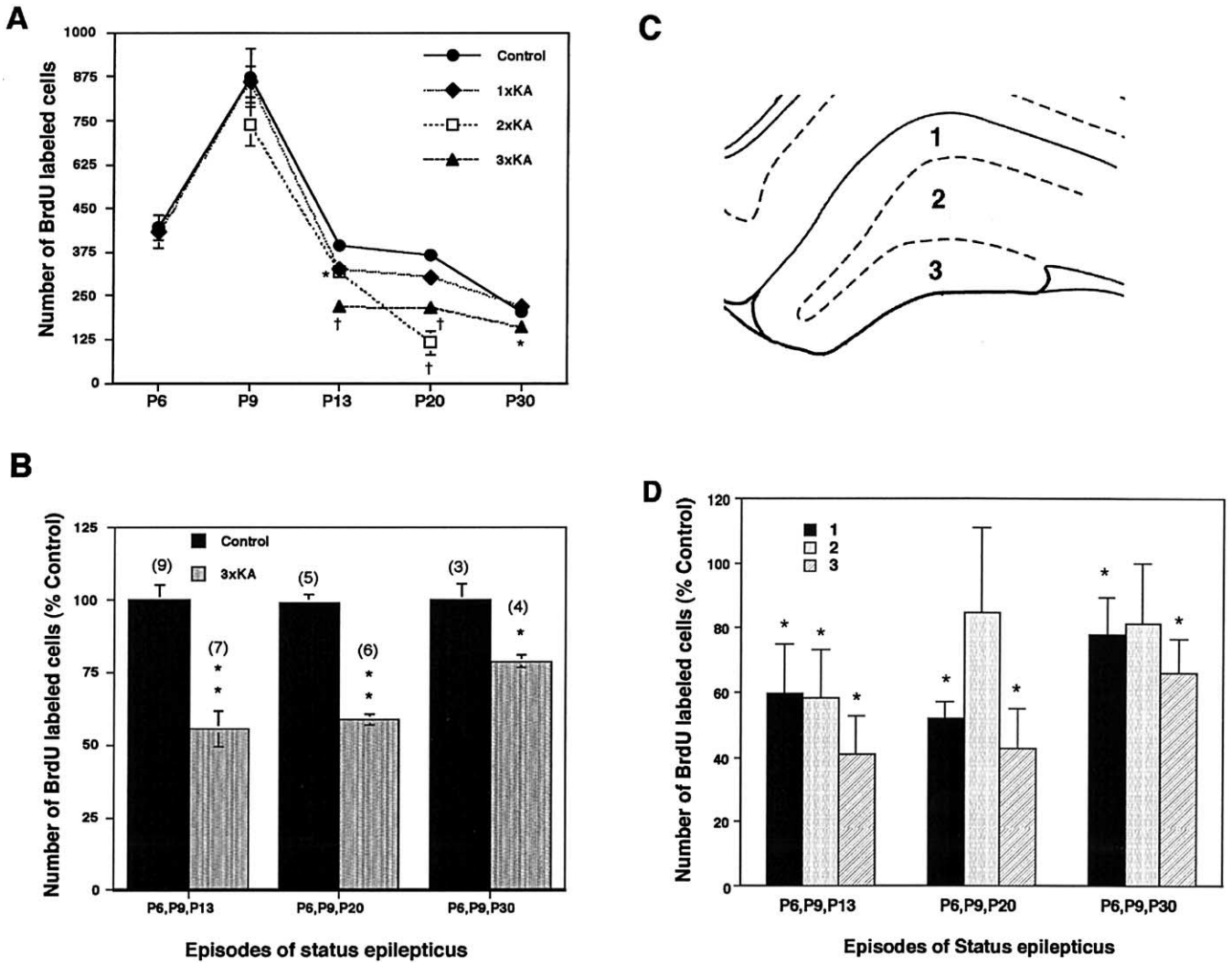

Fig. 2. (A), Quantification of the number of postnatal bromodeoxyuridine (BrdU)-labeled cells of the dentate gyrus after 1 ×, 2 ×, and 3 × Kainete (KA). (B) Percentage of BrdU-labeled cells. (C) Schematic figure of upper (1), hilar (2), and lower blades (3) of the dentate gyrus. (D) Quantification of percentage of BrdU-positive cells distributed within the defined regions 1, 2, and 3 at 48 h after induction of the last KA seizure at the indicated ages. P13 with 3 × KA had significantly reduced BrdU-labeled cells in dentate granule and hilar areas. When the third seizure was induced at a later age (P20 or P30) a significant reduction was found only in the granule cell borders and the difference was greater at P20. Values are expressed as percentage of control in corresponding regions. Error bars represent the standard error of 6–9 animals per group. Two-way and three-way analysis of variance was used for statistical analysis of number of BrdU-labeled cells (*$P < 0.05$; †$P < 0.001$).

seizures (P6, P9, and P13) (dorsal blade: 59.8 ± 15.2% vs. ventral blade: 40.8 ± 11.8% of control, $n = 7$, $P < 0.05$). There was also a significant difference in the BrdU mean values among the different age groups ($F = 30.54$, $P < 0.001$).

After allowing for the effects of different ages and treatment, three-way ANOVA showed that there was a significant difference among the different granule cell layers ($F = 3.49$, $P = 0.028$). The effect of different ages depended upon what layer was analyzed. After allowing for the effects of differences in age and layer, the mean values of different levels of treatment (number of seizure episodes) were significantly altered ($F = 3.46$, $P = 0.007$). Specifically, at P20 or P30 and 3 × KA, a significant reduction in the number of BrdU-labeled cells appeared within the upper and lower blades but not within the hilar region (Fig. 2D). The effect on suppression of newly born cells within the borders was less extensive at P30 relative to the younger age groups exposed to 3 × KA. Thus, there was a significant interaction between age and granule cell layer ($F = 3.49$, $P = 0.018$).

BrdU-labeled cells colocalize with neuronal markers

Double-labeling immunohistochemistry was performed with BrdU and NeuN or BrdU with GFAP antibodies to estimate the percentage of BrdU-labeled cells that were neurons. Only Group III was analyzed since the older ages also received their first two BrdU injections during the peak of hilar proliferation (on P6 and P9). BrdU immunofluorescence was intense and revealed two types of granule cells

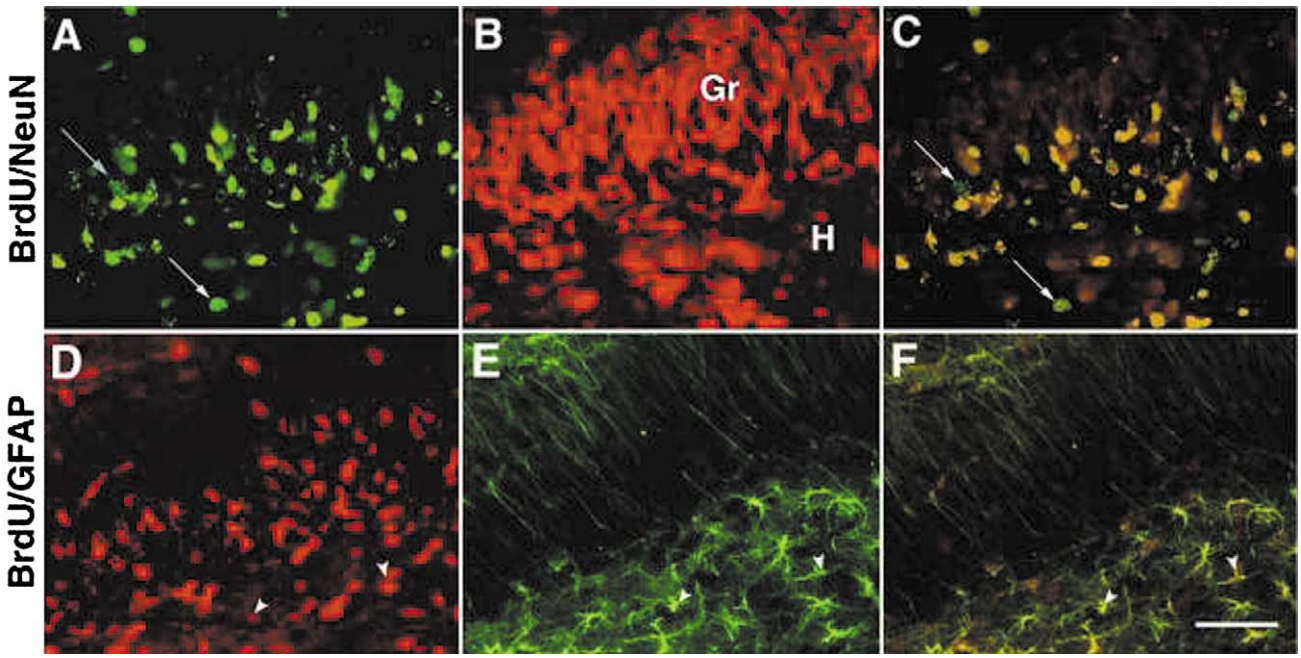

Fig. 3. Double-labeling immunofluorescence of the dentate hilus with bromodeoxyuridine (BrdU) and NeuN or BrdU and GFAP after one Kainate (KA) injection given on P6, P9, and P13, at the level of the hippocampus. Along the hilar border BrdU linked to FITC (A), or to avidin-Texas Red (D), intense labeling of two types of BrdU-labeled cells, i.e., solid nucleus and spherical bodies. (B) NeuN linked to avidin-Texas shows uniform, bright fluorescence of granule cells. (C) Superposition of images of BrdU and NeuN show most cells colocalize and few do not (arrows). (E) GFAP fluorescence shows most glia are located within the hilus and not along the border of the granule/hilar layers. (F) Superposition of images of BrdU and GFAP labeling show few cells coexpress both proteins (arrowheads). Scale bar = 50 μm. Gr, dentate granule cells; H, dentate hilus.

along the hilar border as described above (Fig. 3) and by recent studies (Gould et al., 1997a; McCabe et al., 2001). Double-labeling for glia using GFAP fluorescence showed distinct patterns such that most glia were located within the hilus and not along the molecular layer border of control and experimental animals. However, some BrdU-labeled cells were colabeled with GFAP, indicating that a population of newly dividing cells also included glia (Table 3). Quantification of double-labeled cells of the P13 age group for BrdU and NeuN showed that the majority of BrdU-labeled cells of the subgranular zone were neurons, consistent with other reports (Fig. 3 and Table 3). Because the older age groups (P20 and P30) received their BrdU injections at the same early ages of P6 and P9 as the P13 age group had, and neurogenesis declines as a function of age, then the majority of suppressed cells captured at these older ages are assumed to be from the early insults and are also assumed to be neurons. In keeping with this, minimal damage was detected at this age in this region and time after KA-induced status epilepticus (Nickel and Szelenyi, 1989) and gliosis of the hilus also did not coexist in our study as determined by Nissl and TUNEL staining methods (see below and Fig. 4). Therefore, it appears that neuronal proliferation was affected and it is unlikely that gliosis had any effect on suppressing neurogenesis.

Table 3
Percentage of bromodeoxyuridine (BrdU)-positive cells double-labeled with either NeuN (neuronal marker) or GFAP (glial marker) at P13 (n = 5)[a]

	% BrdU + NeuN		% BrdU + GFAP	
	3 × KA	Control	3 × KA	Control
Upper blade	83.3 ± 3.5	85.1 ± 2.9	12.9 ± 2.2	11.2 ± 2.2
Hilus	11.7 ± 2.3	11.5 ± 2.4	80.1 ± 3.7	79.1 ± 2.9
Lower blade	84.1 ± 2.5	83.8 ± 3.0	13.6 ± 1.7	12.4 ± 1.4

[a] BrdU/NeuN colabeled cells were predominant in the granule cell layers and BrdU/GFAP colabeled cells were predominant in the hilus. There was no difference in the percentage of colabeled cells after seizures. KA, Kainate.

Suppression of neurogenesis is not due to neurodegeneration

To examine whether alterations in neurogenesis corresponded to necrotic or apoptotic cell death mechanisms, histology was performed and brain sections were studied at the light microscopic level in all of the groups. After 1 × or 2 × KA and 48 h after the last seizure, no histological changes of the dentate gyrus were observed at P6 or P9. In P13 pups with 3 × KA, (on P6, P9, and P13), cell death of the dentate gyrus was also not apparent at the light microscopic level, with the degenerating stains tested (i.e., hematoxylin/eosin, thionin, silver, and TUNEL). Eosinophilia was not detected in the inner layer and argyrophilic neurons

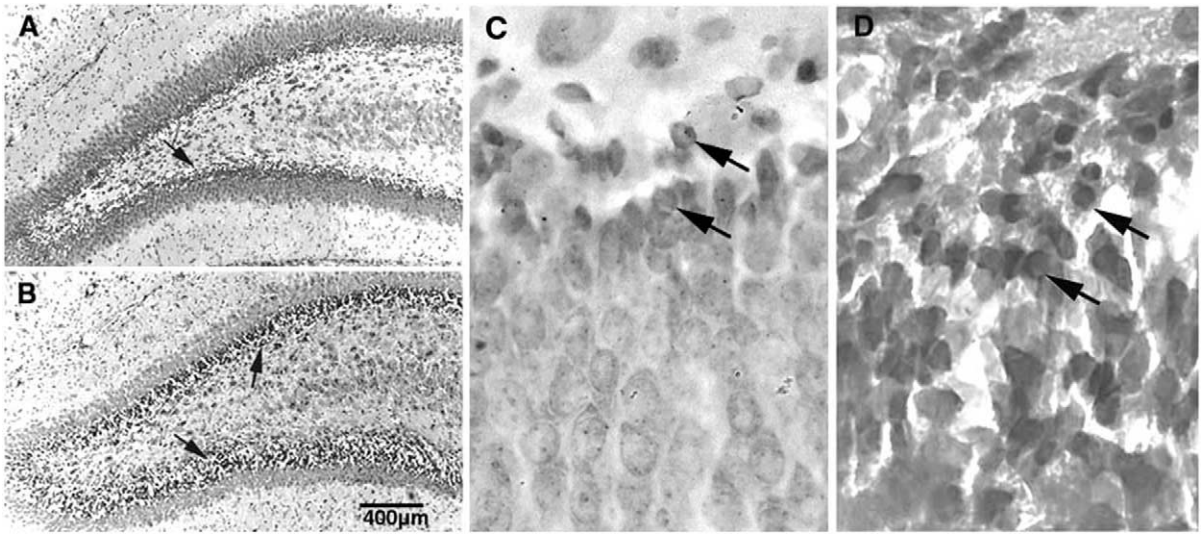

Fig. 4. Histological staining of the P13 dentate gyrus 48 h after 3 × kainate (KA). (A) Phosphate-buffered saline control-injected P13 rats showed normal hematoxylin/eosin staining. Lower arrow points to normal area shown at higher magnification in panels C and D. The granule cell layer appears thick with mature cells lined with immature smaller cells that face the hilar border (arrows). (D) After 3 × KA, hematoxylin/eosin showed many shrunken inner granule cells with increased bluing (hyperbasophilia, arrows) and thickness of the inner layer facing the hilus.

were absent in any part of the dentate gyrus (Fig. 4). However, histological alterations were observed after 3 × KA in the absence of cell death. For example, there was a significant increase in the number of basophilic stained cells at the hilar border of the granule cell layer (PBS: 788 ± 88 vs. 3 × KA: 1306 ± 172, $P < 0.01$). Hematoxylin/eosin also revealed that the granule cell inner layer area significantly increased after 3 × KA relative to 1 × KA or PBS-injected animals (PBS: 0.498 ± 0.066 vs. 3 × KA: 0.831 ± 0.137 mm, $P < 0.01$) (see Fig. 4C and D). In contrast, preferential injury to the CA1 was observed with the four stains used after 1 × KA at P20 and P30 (Fig. 5A and B), similar to pilocarpine injected into immature rats (Sankar et al., 1997). The CA1 damage was highly reduced in these older ages when animals had a history of one or two of the perinatal seizures (unpublished data). Thus, obvious cell death within the dentate gyrus was not correlated with the suppressed number of BrdU-labeled cells.

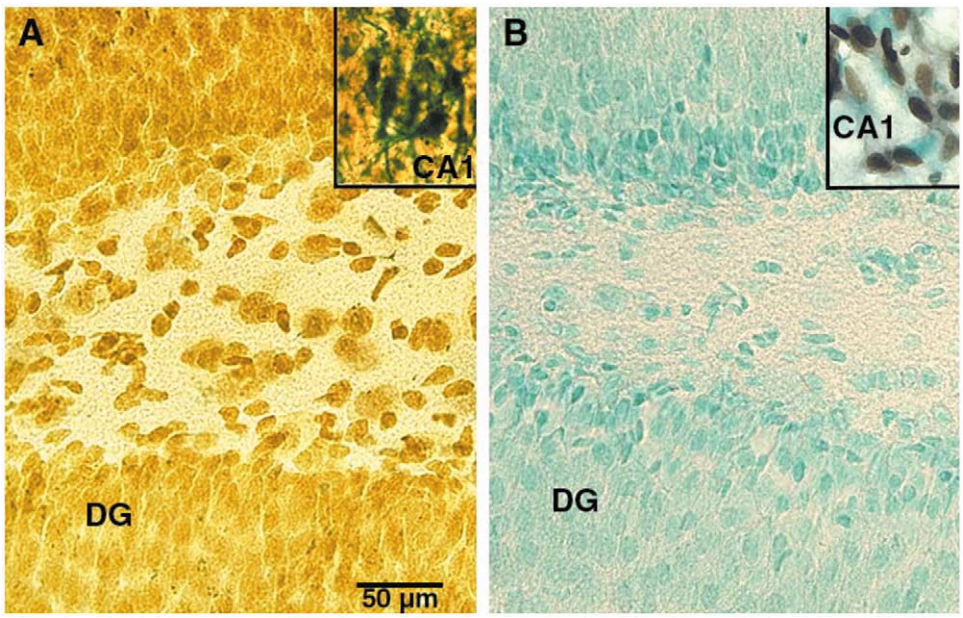

Fig. 5. (A) Silver impregnation and TUNEL staining (B) showed that argyrophilia and TUNEL-positive cells were absent in the inner granule cell layers and hilar regions. There was no obvious gliosis. The CA1 region (the insets in A and B) becomes vulnerable to damage 48 h following 1 × Kainate (KA) in the P20 rats and thus serves as a positive control within the same section where many silver and TUNEL-labeled cells can be found.

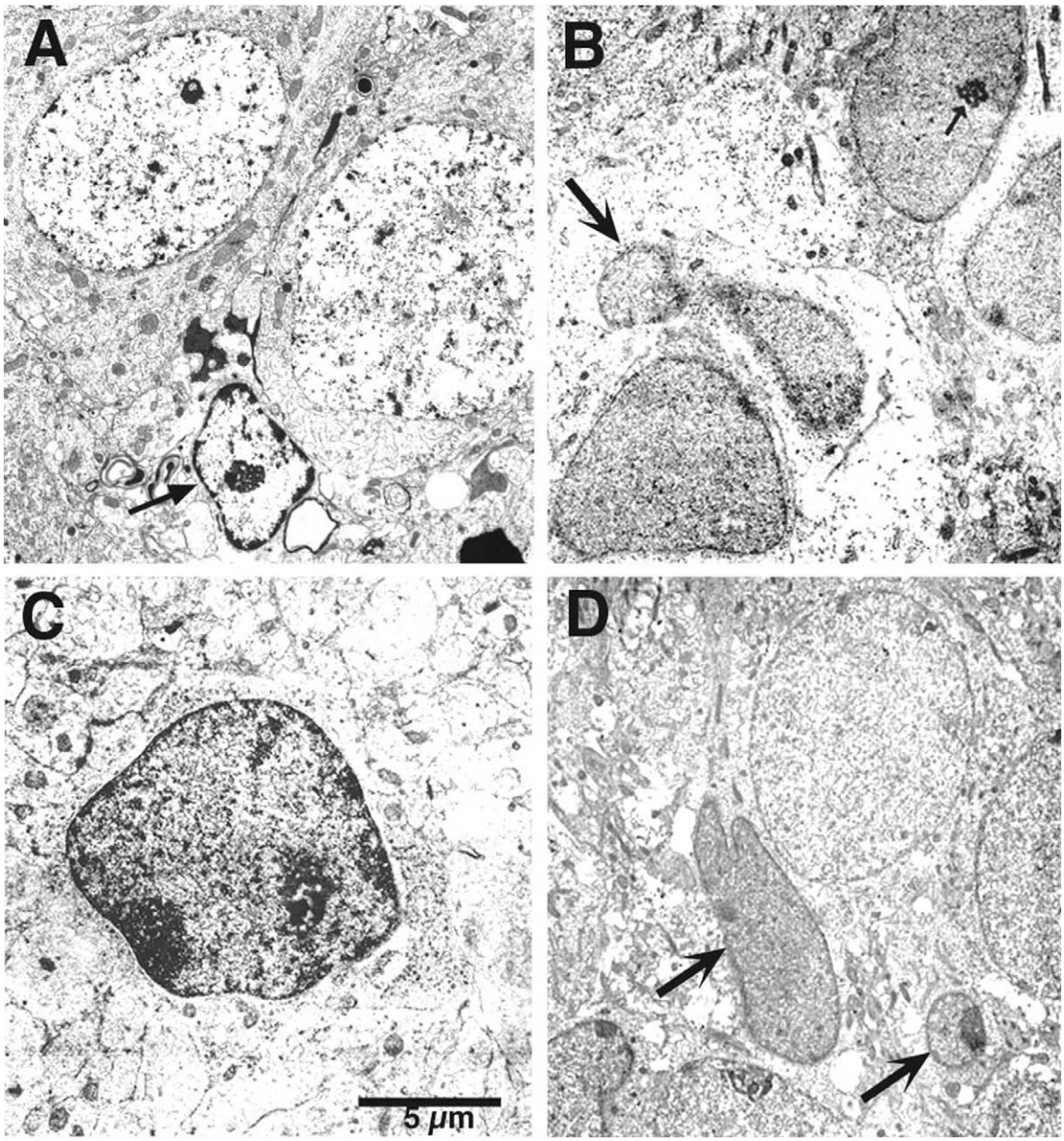

Fig. 6. Electron micrographs at 48 h after three perinatal seizures induced on P6, P9, and P13. (A) Phosphate-buffered saline control showing two mature granule cells with round nuclei (thin arrow) and clear cytoplasm with well-developed organelles. Supporting glial cells were typically observed (arrow). (B) Immature granule cells and putative stem cells are shown with irregular shapes (thick arrows) and electron dense (thick arrows) nuclei at the hilar border of the granule cell layer. The watery cytoplasm of these cells was deprived of well-developed cytosolic organelles. (C) An immature granule cell at the hilar border with irregular shape, increased electron density, and marked chromatin condensation. (D) Irregular shaped immature and putative stem cells (arrows) were immunopositive for bromodeoxyuridine (thick arrows), and intermingled with mature unlabeled cells. Scale bar = 3 μm.

Ultrastructural features of newly generated granule cells

To obtain higher resolution of the granule cell layers than the Nissl-stained sections, semithin and ultrathin sections were prepared for light and electron microscopes. At the ultrastructural level three types of granule cells, mature, immature, and putative stem cells were morphologically identified in PBS control and Group III animals (3 × KA on P6, P9, and P13) (Fig. 6 and Table 4). Immature cells were medium in size with round, oval, or elliptical cell somata (Fig. 6). Mature cells were larger in size and had oval nuclei with round cell bodies, a watery cytoplasm, and well-developed cytosolic organelles as described (Ribak and Navetta, 1994; Seress and Ribak, 1990) (Fig. 6A and D). They were found at the molecular layer border or deep within the granule cell layers. They were postsynaptic to axon terminals and made symmetric synapses. In contrast, immature granule cells were mainly found at the hilar border of the granule cell layer but they lacked glial support cells. The immature cells had increased electron-dense nuclei and

Table 4
Electron microscopy of the dentate gyrus after 3 × Kainate (KA) on P6, P9, and P13[a,b]

	Mature	Immature	Stem	*N*
PBS	108.3 ± 19.9	45.3 ± 12.7	15 ± 2.08	3
3 × KA	65.3 ± 6.1[c]	61.3 ± 7.5	64.3 ± 27.2[c]	3

[a] After 3 × KA, electron microscopy showed that there were an increased number of immature putative stem cells and decreased number of mature granule cells. Values represent actual cell numbers. Mature and immature granule cells and putative stem cells lining the hilar/granule cell borders were counted from at least four grids at random with an electron microscope. PBS, phosphate-buffered saline.

[b] Two-way analysis of variance $F = 97.4 = P < 0.001$, and χ^2 nonparametric tests were used for statistical analysis

[c] ($P < 0.01$).

were deprived of well-developed cytosolic organelles. The putative stem cells were very small in size, had an electron dense nucleus, and were irregular in shape (Fig. 6A and B). The putative stem cells were found in the subgranular zone of the hilus and often were mixed in with the immature granule cells. The number of each cell type varied significantly and some appeared to be dividing (Fig. 6B).

At 48–72 h after the third seizure induced on P13 (Group III), there were a similar proportion of cell types (Table 4). EM showed that there were an increased number of immature putative stem cells and decreased number of mature granule cells. Many cells were small in size with a darkened cytoplasm, resembling an immature state (Fig. 6B). EM occasionally showed other irregular cells located within the hilus with increased chromatin condensation (Fig. 6C). After cells were immunolabeled for BrdU at the EM level, they were first identified in semithin plastic sections as having brown colored nuclei. Their identification by EM was confirmed by correlating their location and distribution and then compared with PBS controls (Fig. 6D). In addition, these labeled cells contained electron-dense reaction product within their nuclei and had similar irregular morphological features as the immature and putative stem cells (Fig. 6A, E, and F). Two-way ANOVA showed that the difference in the mean values among the different cell types was significantly altered after allowing for effects of differences in treatment ($F = 97.4$, $P < 0.001$; Table 4). Due to a small n for EM studies, the χ^2 test of independence was also performed and this test also showed that the population of cell type was significantly related to the treatment (i.e., number of seizures, $\chi^2 = 62.919$, $DF = 8$, $P < 0.001$). After averaging all granule cell types and calculating the percentage for individual types, there was a significant decrease in the percentage of mature granule cells after 3 × KA (Group III) relative to control and an increase in the percentage of immature and putative stem cells relative to control (Fig. 7). There was a statistically significant interaction between cell type and treatment, such that the effect on the different number of cell types was dependent upon the number of KA seizures ($F = 112.8$, $P < 0.001$). Thus, the proportion of cell type was significantly related to the treatment. Moreover, mature granule cells were BrdU-immunonegative at the time point examined, further indicating that the putative and immature granule cells were predominantly affected by the seizures.

Suppression of neurogenesis is related to elevated CORT levels induced by multiple perinatal seizures

Because an inverse relationship exists between CORT levels and granule cell proliferation, plasma CORT levels were measured at times after the last seizure to elucidate underlying mechanisms that inhibit cell proliferation. At P6 in control PBS-injected animals, basal CORT levels were low (0.06 ± 0.1 μg/dl), increased steadily until P15, then rose sharply between P20 and P22, and declined at P30 (Fig. 7A). CORT plasma levels were negatively correlated with the number of BrdU-labeled cells as a function of age ($r = -0.90$, $P < 0.05$) (Fig. 8A). At P6 and after one episode of KA-induced status epilepticus (Group I), a biphasic response was observed such that circulating CORT levels first increased (to 2.40 ± 0.86 μg/dl) and reached a peak at 1–2 h after the KA injection. Control CORT levels were observed at 4 h and significant rises reappeared at 8 h then remained significantly elevated above baseline at 48 and 72 h after the KA injection (Fig. 8B). At P9 and 2 × KA (Group II), CORT levels were increased to 10.5 ± 0.78 μg/dl after 1 h and remained significantly elevated at 4 and 8 h after KA injection and then returned to baseline by 24 h (Fig. 8C). In contrast, P9 pups exposed to 1 × KA had baseline levels of CORT 8 h after KA injection, suggesting that the P6 seizure induced earlier may have had a cumulative effect (P9, 1 × KA, and 8 h: 0.68 ± 0.039, $n = 6$ vs. 2 × KA and 8 h: 2.73 ± 0.68 μg/dl $n = 5$, $P < 0.001$). At

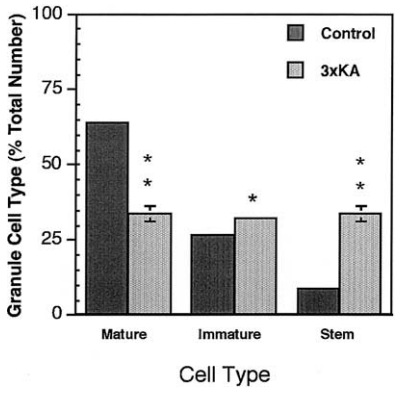

Fig. 7. Quantification of the number of three types of granule cells of the dentate gyrus in control P15–16 pups and after 3 × Kainate (KA). Two-way analysis of variance and χ^2 of independence test were used for statistical analysis and showed that the difference in the mean values among the different cell types was significantly altered after allowing for effects of differences in treatment (*$P < 0.05$; **$P < 0.001$).

P13 and 3 × KA (Group III), plasma CORT levels also increased to 12.3 ± 0.76 μg/dl, remained in that range at 4 h, and returned to baseline at 24 h (Fig. 8C). At P20 and 3 × KA (Group IV), CORT elevations were high (30.3 ± 0.61 μg/dl) relative to the younger ages at 1 h and also significantly elevated at 4 h (17.4 ± 0.59 μg/dl). This was similar to control total CORT plasma levels measured on P22 (16.2 μg/dl), an age associated with reduced neurogenesis in normal development. Interestingly, at 2, 4, or 8 h after KA, the raised CORT level, measured as a percentage of baseline, was high above baseline for all of the age groups examined, particularly those with a history of at least one early perinatal seizure induced during the peak of neurogenesis (Fig. 8D). Elevated levels of CORT after 3 × KA at 1–4 h or 24–72 h were not significantly correlated with the natural decline in the number of BrdU-labeled cells that occurs with age ($r = -0.6$, $P > 0.05$). Therefore, measurement of total circulating plasma CORT levels showed that there were postictal increases associated with suppression of cell proliferation induced by the earlier neonatal seizures.

Discussion

Suppression of neurogenesis depends upon age and seizure history

The present study showed that three episodes of sustained status epilepticus within the first 13 days of postnatal life dramatically suppress neurogenesis of granule cells in the dentate gyrus during active phases of their proliferation and migration. In addition, a history of only one or two perinatal seizure(s) can suppress hippocampal neurogenesis if a second or third seizure recurs after a critical developmental period at P20, an age associated with a sharp but transient surge in CORT. The negative correlation observed between the number of BrdU-labeled cell counts and total CORT levels was lost in Groups III–V due to the reduced number of BrdU-labeled cells induced by several perinatal KA seizures. Because these groups had the greatest number of BrdU injections (four), it is improbable that the BrdU-labeling was diluted to account for the decrease. Onset of seizures during the early perinatal period is supported as a critical factor, because a delayed reduction in cell proliferation also occurs when generalized motor seizures by flurothyl are initiated within the first 5 days of postnatal life (McCabe et al., 2001). In contrast, rat pups exposed to lithium-pilocarpine seizures, after a critical period beginning at 2 or 3 weeks postnatal, showed increased cell division of the subgranular proliferative zone (Sankar et al., 2000) similar to the adult pattern (Gray and Sundstrom, 1998; Parent et al., 1997, 1998; Scott et al., 1998). Therefore, the seizure paradigm employed, the number of seizures, and the age at which seizures are first initiated affect the total proliferation of granule cells of the hippocampus.

Glucocorticosteroids correlate with suppression of neurogenesis

The postnatal limbic-hypothalamic-pituitary-adrenal axis (LHPA) in the immature rodent is different from the adult (Vazquez, 1998). Previous studies have shown that adrenocorticotrophic hormone (ACTH) and CORT plasma levels are developmentally regulated such that they increase significantly on P14 and again on P21 (Vazquez, 1998) similar to our observations. Consequently, the first 12 days of postnatal development in the rodent was considered as a hyporesponsive period to stress whereby rises in CORT levels are limited relative to adults (De Kloet et al., 1988). However, our study also showed that CORT levels decline by P30 prior to puberty, suggesting that high levels of CORT peak during a critical period that was associated with the highest reductions in neurogenesis (P13–P20).

Because there is an established inverse relationship between the endogenous surge of circulating CORT levels and neurogenesis (Sapolsky and Meaney, 1986; Schlessinger et al., 1975), we hypothesized that CORT levels may be elevated for a prolonged period by the earlier perinatal seizures. Accordingly, CORT levels increased significantly at P6 and 1 × KA, and responses were sustained for over 4 h at P9 and 2 × KA. Neurogenesis was not suppressed at these ages possibly because CORT levels did not reach the minimal level required (10–15 μg/dl) to interfere with cell division. In contrast, reduced neurogenesis was observed in four of the older groups, P13, P20, or P30 ages with 3 × KA (Groups III, IV, and V), and P20 with only 2 × KA (Group IV). This may be due to the enhanced surge of CORT observed at this critical age, which is assumed to surpass the level of CORT required to inhibit neurogenesis akin to that observed during the natural course of normal development. The data suggest that early perinatal rises in CORT after 1 × or 2 × KA on P6 and P9, respectively, may have cumulative inhibitory effects during the height of granule cell proliferation that were insufficient to induce a reduction in BrdU cell counts until a third seizure was induced. The data also suggest that the sharp rise in CORT at P20–P22 may have been sufficient to inhibit neurogenesis with only one previous perinatal seizure and could explain why a certain number of seizures or age reached was necessary to observe the inhibition of granule cell neurogenesis. Although higher levels of CORT were found with increasing age and with increasing perinatal seizures, it should also be noted that naturally occurring changes in steroid levels may be offset by corticosteroid binding globulin (CBG) concentrations (Viau et al., 1996). For example, CBG levels are low to absent in the P6 animals of our study and raised at the older ages, which may influence the suppression of neurogenesis (Viau et al., 1996). On the other hand, no significant correlation was found between total cortisol and CBG levels

in human neonates with varying birth weights or health conditions (Hanna et al., 1997; Kari et al., 1996). However, KA-induced perinatal seizures may effect CBG levels; therefore, hormone manipulation experiments are in progress to normalize CORT levels prior to seizure induction to further elucidate whether CORT is the main player in the inhibition and whether elevated CORT levels for a sustained period at the younger ages are biologically relevant.

Studies supporting a role for adrenal steroids in adult rat epilepsy models show that plasma adrenalcorticosteroid (ACTH), corticosterone, and β-endorphin levels are elevated in response to kindled seizures and the concentrations are higher with repeated kindling (Young et al., 1990). In addition, corticosterone supplements administered to adult animals not only augment KA-induced seizure automatisms (Lee et al., 1989) and subsequent damage (Sapolsky et al., 1985), but also enhance KA-induced electrophysiopathological changes in the hippocampus that are blocked by the selective CORT antagonist, RU486 (Talmi et al., 1995). Similarly, adrenalectomy performed in adult animals stimulates progenitors and their progeny (Cameron and McKay, 1999). On the other hand, stress also stimulates glucocorticoid responses but decreases neurogenesis in either mature or immature animals (Gould and Tanapat, 1997, 1999; Gould et al., 1998), suggesting that steroid responses may have differential effects on neurogenesis in the immature vs. mature brain. Interestingly, corticosteroid administration by Andreatini and Leite (1994) did not alter seizures induced by a GABAergic antagonist, pentylenetetrazol (PTZ). This implies that direct activation of glutamate receptors may be critical to the corticosteroid response and that not all types of seizures may affect neurogenesis. It should be noted that hypoxia could not explain the age-dependent inhibition of neurogenesis, because the imposed delay of KA injections, between the first perinatal seizure on P6 and P20 or P30, was too long to cause adverse effects that oxygen deprivation may have on cell division. Similarly, Wasterlain showed dissociation between anoxia and electroconvulsive shock seizures; elicited within the first 11 days of postnatal development because smaller brains and reduced DNA content was not apparent until animals matured to P30 (Wasterlain, 1976; Wasterlain and Plum, 1973). Finally, more extreme loss of oxygen produced by global ischemia can enhance cell proliferation in the mature dentate gyrus (Kee et al., 2001).

Disturbance of newly born granule cell migration

Newborn granule cells were proposed to give rise to mossy fiber sprouting that follows status epilepticus in adults (Parent et al., 1997). This was later refuted by irradiation studies whereby progenitors were selectively killed but without any noticeable effect on synaptic reorganization (Parent et al., 1999). However, age-dependent aberrant connections may be pertinent if migration of newly born granule cells into the granule cell layer is altered by perinatal seizures before cells are fully committed. In Groups IV and V (P20 or P30), the number of BrdU-labeled cells located within the hilus was unaltered in animals with a history of three perinatal seizures, but only cells that had migrated to the upper and lower blades were reduced; hilar cell number was unaffected. This supports the hypothesis that the ones most vulnerable to the seizure insult were progenitors undergoing cell division earlier and were in an active phase of migration. Interestingly, EM showed that three neonatal seizures increased the proportion of immature and putative stem cells that lacked glial support cells, further suggesting that migration of new granule into maturing granule cells was likely impaired.

Abnormal migration of granule cell progenitors and progeny occurs in mature animals in that BrdU-labeled neurons ectopically appear in the CA3/hilus several weeks after status epilepticus (Scharfman et al., 2000). However, in sections from Group III pups, some cells at the ultrastructural level still appeared to be dividing. This suggests that the newly born cells may continue to proliferate, overaccumulate, and not differentiate into mature granule cells, therefore remaining in an immature state. Because more than one episode of status epilepticus was required to alter the morphology of granule cell progenitors, retardation of cell maturation may be due to the repeated increases in CORT levels induced by the earlier perinatal seizure(s) that could interfere with the S phase of the cell cycle.

Other mechanisms of suppression

Maturational differences in NMDA receptor expression and function may also explain why lesions produced by pilocarpine seizures (Parent et al., 1997) or excitotoxins (Gould et al., 1997a) stimulate neurogenesis in adults. For example, inhibition of granule cell neurogenesis at P13–P20 coincides with a time when hippocampal NMDA receptors are transiently upregulated (Monyer et al., 1991, 1994). During this developmental period, apical dendrites of CA1 pyramidal neurons are most sensitive to NMDA application, expressed by large influxes of calcium (Hamon and Heinemann, 1988). In adult rats, NMDA application blocks adrenalectomy-induced increases in neurogenesis (Cameron et al., 1998). Similarly, treatment with the NMDA receptor antagonist MK-801 prevents corticosteroid-induced neuroprotection (Cameron et al., 1998). However, an age-dependent NMDA receptor-mediated factor is not supported, because Gould and Cameron (1997) also showed that rat pups treated with different doses of the NMDA receptor antagonist CGP 43487 on P5 had a dose-dependent increase in the number of [^{3}H]thymidine-labeled cells in the dentate gyrus. An inverse relationship between cell proliferation and NMDA receptor blockade and steroid synthesis in both mature and immature animals obscures interpretation as to why seizures induce opposite effects on neurogenesis with maturation. Moreover, a lesion of the entorhinal cortex also

stimulates neurogenesis of the dentate gyrus (Cameron et al., 1995). Thus, an alternate explanation to suppression is that seizure-induced deafferentation of excitatory inputs to the hippocampus does not appear until after the third postnatal week (Nitecka et al., 1984). Another possibility is likely due to maturational differences that seizures have on neuronal and basic fibroblast growth factors (e.g., NGF, BDNF, and bFGF), which are stimulated by seizures in adults (Isackson et al., 1991) but not in pups (Dugich-Djordjevic et al., 1992). Accordingly, injections of bFGF into immature or mature animals significantly enhance dentate granule cell neurogenesis (Wagner et al., 1999). Insulin-like growth factor-1 has also been shown to increase neurogenesis in the adult brain (Aberg et al., 2000). In our study, TUNEL, silver impregnation, and EM did not reveal necrosis or apoptosis of neurons in the granule cell layer at times of suppressed neurogenesis. Therefore, some unknown factor that may be secreted by degenerating cells is probably not involved in the cell suppression of neurogenesis.

Seizure activity and clinical implication

A role for neurogenesis in seizure susceptibility is improbable due to the opposite effects that perinatal seizures had on neurogenesis and high-frequency synchronous events in the EEG. For example, ictal activity was increased in Group III rats but reduced in Groups IV and V animals with the same history of perinatal seizures. BrdU-labeling was inhibited despite decreases in synchronized activities in the EEG and increased maturation of the animals. In addition, one episode of sustained status epilepticus had no

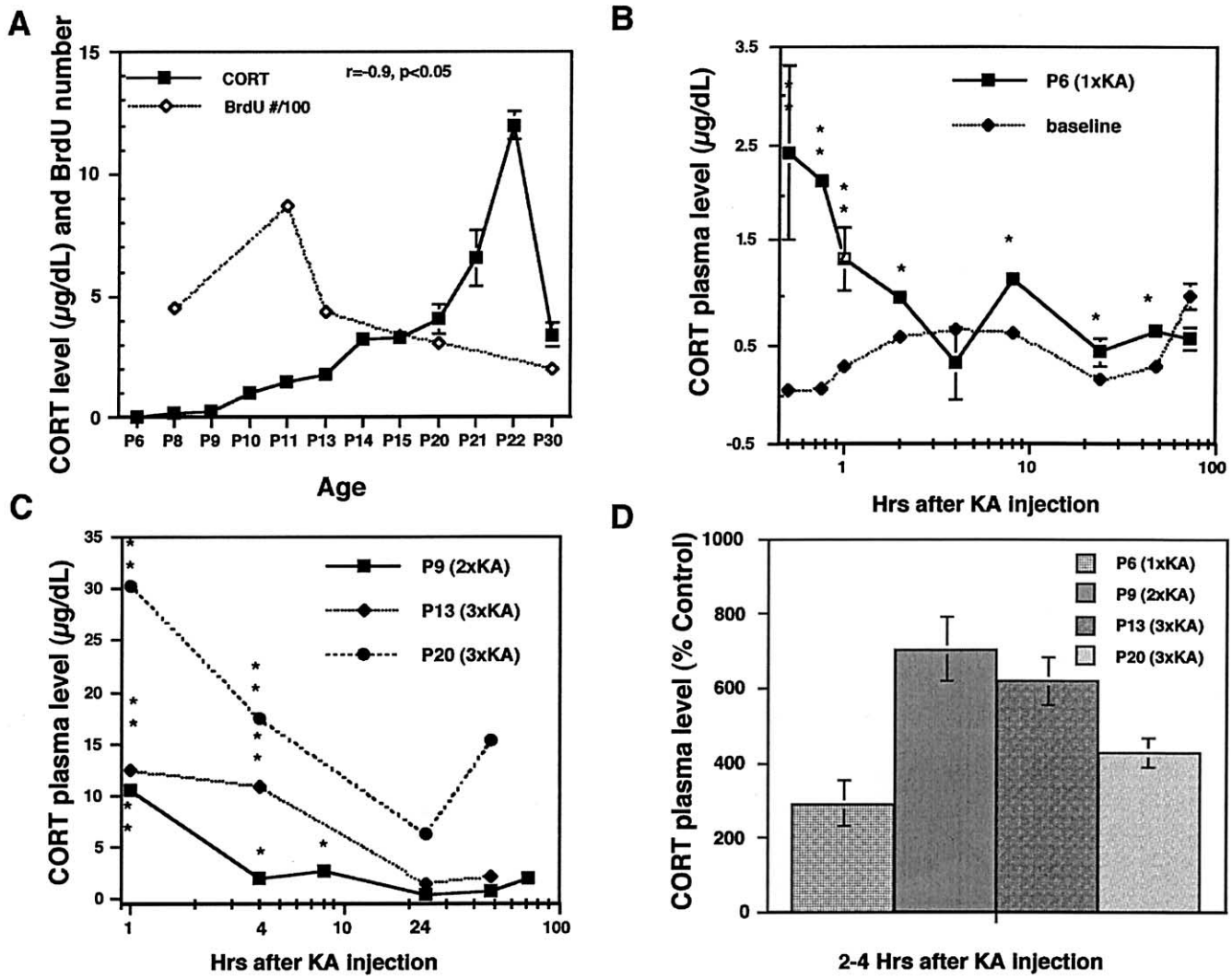

Fig. 8. Plasma glucocorticosteroid (CORT) levels were measured as micrograms per deciliter (μg/dl) (mean ± SEM) from age-matched controls and after 1 ×, 2 ×, and 3 × Kainate (KA) experimental conditions. (A) Developmental increases in plasma CORT levels correlated with bromodeoxyuridine (BrdU) number (divided by 100) as a function of age ($r = 0.9$, $P < 0.05$). A sharp rise in CORT occurs between P20 and P22 and declines at P30. (B) Acute increases in CORT levels were sustained for a prolonged period at P6. (C) CORT levels elevated after 2 × or 3 × KA with higher responses with increasing age. (D) Increased percentage of CORT levels are shown at 2 h for P6 and 4 h for P9, P13, and P20. (*$P < 0.05$; **$P < 0.001$).

effect on newly born cell proliferation at the ages examined. Therefore, there was no apparent relationship between high-frequency ictal activity and suppression of neurogenesis. There are clinical implications because reduction in granule cell proliferation as a result of only two or three perinatal seizures would presumably induce loss of neuronal function with maturation in agreement with others (Holmes et al., 1988). Consequently, suppression of neurogenesis by seizures may be a source for learning deficits in children with epilepsy due to lack of mature hippocampal circuitry. Interestingly, an enriched learning environment (Gould et al., 1999a) and physical exercise (van Pragg et al., 1999) are associated with enhanced granule cell neurogenesis. Since learning stimulates neurogenesis, it remains to be elucidated whether environmental stimuli such as pervasive teaching and exercise tasks may reduce long-term deleterious side effects produced by perinatal seizures.

Acknowledgments

This study was supported by the National Institutes of Health NS-38069 (to L.K.F.) and NS-38331 (to C.E.R). We are grateful to Dr. Robert Keesey for his expert assistance with statistical analysis.

References

Aberg, M.A., Aberg, N.D., Hedbacker, H., Oscarsson, J., Eriksson, P.S., 2000. Peripheral infusion of IGF-1 selectively induces neurogenesis in the adult rat hippocampus. Neuroscience 20, 2896–2903.

Albala, B.J., Moshe, S.L., Okada, R., 1984. Kainic-acid-induced seizures: a developmental study. Dev. Brain Res. 13, 139–148.

Altman, J., Das, G.D., 1965. Autoradiographic and histological evidence of postnatal hippocampal neurogenesis in rats. J. Comp. Neurol. 124, 319–335.

Andreatini, R., Leite, J.R., 1994. The effect of corticosterone in rats submitted to the elevated plus-maze and to pentylenetetrazol-induced convulsions. Prog. Neuropsychopharmacol. Biol. Psychiatry 18, 1333–1347.

Bayer, S.A., 1980. Quantitative ^{3}H-thymidine radiographic analyses of neurogenesis in rat amygdala. J. Comp. Neurosci. 194, 850–875.

Beato, M., Chalepakis, G., Schauer, M., Slater, E.P., 1989. DNA regulatory elements for steroid hormones. J. Steroid Biochem. 32, 737–747.

Cameron, H.A., McEwen, B.S., Gould, E., 1995. Regulation of adult neurogenesis by excitatory input and activation of NMDA receptor activation in the dentate gyrus. J. Neurosci. 15, 4687–4692.

Cameron, H.A., McKay, R.D., 1999. Restoring production of hippocampal neurons in old age. Nat. Neurosci. 10, 894–897.

Cameron, H.A., Tanapat, P., Gould, E., 1998. Adrenal steroids and N-methyl-D-aspartate receptor activation regulate neurogenesis in the dentate gyrus of adult rats through a common pathway. Neuroscience 82, 349–354.

Clayton, C.J., Grosser, B.I., Stevens, W., 1977. The ontogeny of corticosterone and dexamethasone receptors in rat brain. Brain Res. 134, 445–453.

Dallman, M.F., Levin, N., Cascio, C.S., Akana, S.F., Jacobson, L., Kuhn, R.W., 1989. Pharmacological evidence that inhibition of diurnal adrenocorticotropin secretion by corticosteroids is mediated via type 1 corticosterone-preferring receptors. Endocrinology 124, 2844–2850.

De Kloet, E.R., Ratka, A., Reul, J.M., Sutano, W., Van Ekelen, J.A.M., 1987. Corticosteroid receptor types in the brain: regulation and putative function, in: Ganong, W.F., Dallman, M.F., Roberts, J.L. (Eds.), The Hypothalamic-Pituitary-Adrenal Axis Revisited, Annals of the New York Academy of Science, New York, pp. 402–414.

De Kloet, E.R., Rosenfeld, P., van Ekelen, J.A.M., Sutano, W., Levine, S., 1988. Stress, glucocorticoids and development. Boer, G.J., Feenstra, M.P.G., Mirmiran, M., Swaab, D.F. (Eds.). Pro Brain Res. 73, 101–120.

del Rio, J.A., Soriano, E., 1989. Immunocytochemical detection of 5′ bromodeoxyuridine incorporation in the central nervous system. Dev. Brain Res. 49, 311–317.

Dugich-Djordjevic, M.M., Tocco, G., Willoughby, D.A., Najm, I., Pasinetti, G., Thompson, R.F., Baudry, M., Lapchak, P.A., Hefti, F., 1992. BDNF mRNA expression in the developing rat brain following kainic acid-induced seizure activity. Neuron 8, 1127–1138.

Eriksson, P.S., Perfilieva, E., Bjork-Eriksson, T., Alborn, A.M., Nordberg, C., Peterson, D.A., 1998. Neurogenesis in the adult human hippocampus. Nat. Med. 4, 1313–1317.

Friedman, L.K., Sperber, E.F., Moshé, S.L., Bennett, M.V.L., Zukin, R.S., 1997. Developmental regulation of glutamate and $GABA_A$ receptor gene expression in rat hippocampus following kainate-induced status epilepticus. Dev. Neurosci. 19, 529–542.

Gallyas, F., Wolff, J.R., Bottcher, W.H., Zaborszky, L., 1980. A reliable and sensitive method to localize terminal degeneration and lysosomes in the central nervous system. Stain Technol. 55, 299–306.

Gould, E., Beylin, A., Tanapat, P., Reeves, A., Shors, T.J., 1999a. Learning enhances adult neurogenesis in the hippocampal formation. Nat. Neurosci. 2, 260–265.

Gould, E., Cameron, H.A., 1997. Early NMDA receptor blockade impairs defensive behavior and increases cell proliferation in the dentate gyrus of developing rats. Behav. Neurosci. 111, 49–53.

Gould, E., Cameron, H.A., Daniels, D.C., Wooley, C.S., McEwen, B.S., 1992. Adrenal hormones suppress cell division in the adult dentate gyrus. J. Neurosci. 12, 3642–3650.

Gould, E., Cameron, H.A., McEwen, B.S., 1994. Blockade of NMDA receptors increases cell death and birth in the developing rat dentate gyrus. J. Comp. Neurol. 340, 551–565.

Gould, E., McEwen, B.S., Tanapat, P., Galea, L.A.M., Fuchs, E., 1997b. Neurogenesis in the dentate gyrus of the adult tree shrew is regulated by psychosocial stress and NMDA receptor activation. J. Neurosci. 17, 2492–2498.

Gould, E., Reeves, A.J., Fallah, M., Tanapat, P., Gross, C.G., Fuchs, E., 1999b. Hippocampal neurogenesis in adult Old World primates. Proc. Natl. Acad. Sci. USA 96, 5263–5267.

Gould, E., Tanapat, P., 1997. Lesion-induced proliferation of neuronal progenitors in the dentate gyrus of the adult rat. Neuroscience 80, 427–436.

Gould, E., Tanapat, P., 1999. Stress and hippocampal neurogenesis. Biol. Psychol. 46, 1472–1479.

Gould, E., Tanapat, P., Cameron, H.A., 1997a. Adrenal steroids suppress granule cell death in the developing dentate gyrus through an NMDA receptor-dependent mechanism. Dev. Brain Res. 1, 91–93.

Gould, E., Tanapat, P., McEwen, B.S., Flugge, G., Fuchs, E., 1998. Proliferation of granule cell precursors in the dentate gyrus of adult monkeys is diminished by stress. Neurobiology 95, 3168–3171.

Gundersen, H.J., Bendtsen, T.F., Korbo, L., Marcussen, N., Moller, A., Nielsen, K., Nyengaard, J.R., Pakkenberg, B., Sorensen, F.B., Vesterby, A., 1988. Some new, simple and efficient stereological methods and their use in pathological research and diagnosis [review]. A.P-.M.I.S. 96, 379–394.

Gray, W.P., Sundstrom, L.E., 1998. Kainic acid increases the proliferation of granule cell progenitors in the dentate gyrus of the adult rat. Brain Res. 790, 52–59.

Hamon, B., Heinemann, U., 1988. Developmental changes in neuronal sensitivity to excitatory amino acids in area CA1 of the rat hippocampus. Brain Res. 466, 286–290.

Hanna, C.E., Jett, P.L., Laird, M.R., Mandel, S.H., LaFranchi, S.H., Reynolds, J.W., 1997. Corticosteroid binding-globulin, total serum cortisol, and stress in extremely low-birth-weight infants. Am. J. Perinatol. 14, 201–204.

Hildebrandt, K., Teuchert-Noodt, G., Dawirs, R.R., 1999. A single perinatal dose of methamphetamine suppresses dentate granule cell proliferation in adult gerbils which is restored to control values by acute doses of haloperidol. J. Neural Transm. 106, 549–558.

Holmes, G.L., Gairsa, J.L., Chevassus-Au-Louis, N., Ben-Ari, Y., 1998. Consequences of perinatal seizures in the rat: morphological and behavioral effects. Ann. Neurol. 44, 845–857.

Holmes, G.L., Thompson, J.L., Marchi, T., Feldman, D.S., 1988. Behavioral effects of kainic acid administration on the immature brain. Epilepsia 29, 721–730.

Isackson, P.J., Huntsman, M., Murray, K.D., Gall, C.M., 1991. BDNF mRNA expression is increased in adult rat forebrain after limbic seizures: temporal patterns of induction distinct from NGF. Neuron 6, 937–948.

Kari, M.A., Ravio, O., Stenman, U.H., Voutilainen, R., 1996. Serum cortisol, dehydropiandrosterone sulfate, and steroid-binding globulins in preterm neonates: effect of gestational age and dexmethasone therapy. Pediatr. Res. 40, 319–324.

Kawata, M., Yuri, K., Ozawa, H., Nishi, M., Ito, T., Hu, Z., Lu, H., Yoshida, M., 1998. Steroid horomones and their receptors in the brain. J. Steroid Biochem. Mol. Biol. 65, 273–280.

Kee, N.J., Preston, E., Wojtowicz, J.M., 2001. Enhanced neurogenesis after transient global ischemia in the dentate gyrus. Exp. Brain Res. 136, 313–320.

Kempermann, G., Kuhn, H.G., Gage, F.H., 1997. More hippocampal neurons in adult mice living in an enriched environment. Nature 386, 493–495.

Kornack, D.R., Rakic, P., 1999. Continuation of neurogenesis in the hippocampus of the adult macaque monkey. Proc. Natl. Acad. Sci. USA 96, 5768–5773.

Kuhn, H.G., Dickinson-Anson, H., Gage, F.H., 1996. Neurogenesis in the dentate gyrus of the adult rat: age related decrease of neuronal progenitor proliferation. J. Neurosci. 16, 2027–2033.

Lee, P.H., Grimes, L., Hong, J.S., 1989. Glucocorticoids potentiate kainic acid-induced seizures and wet dog shakes. Brain Res. 480, 322–325.

Malberg, J.E., Eisch, A.J., Nestler, E.J., Duman, R.S., 2000. Chronic antidepressant treatment increases neurogenesis in adult rat hippocampus. J. Neurosci. 20, 9104–9110.

McCabe, B.K., Diosely, S.C., Cilio, M.R., Ho Cha, B., Liu, X., Sogawa, Y., Holmes, G., 2001. Reduced neurogenesis after perinatal seizures. J. Neurosci. 21, 2094–2103.

McEwen, B.S., Weis, J.M., Schwartz, L.S., 1969. Uptake of corticosterone by rat brain and its concentration by certain limbic structures. Brain Res. 16, 227–241.

Monyer, H., Burnashev, N., Laurie, D.J., Sakmann, B., Seeburg, P.H., 1994. Developmental and regional expression in the rat brain and functional properties of four NMDA receptors. Neuron 3, 529–540.

Monyer, H., Seeburg, P.H., Wisden, W., 1991. Glutamate-operated channels: Developmentally early and mature forms arise by alternative splicing. Neuron 6, 799–810.

Morimoto, M., Morita, N., Ozawa, H., Yokoyama, K., Kawata, M., 1996. Distribution of glucocorticoid receptor immunoreactivity and mRNA in the rat brain: an immunohistochemical and in situ hybridization study. Neurosci. Res. 26, 235–269.

Nickel, B., Szelenyi, I., 1989. Comparison of changes in the EEG of freely moving rats induced by enciprazine, buspirone and diazepam. Neuropharmacology 28, 799–803.

Nitecka, L., Tremblay, E., Charton, G., Bouillot, J.P., Berger, M.L., Ben-Ari, Y., 1984. Maturation of kainic acid seizure brain damage syndrome in the rat. II. Histopathological sequelae. Neuroscience 13, 1073–1094.

Nowakowski, R.S., Rakic, P., 1981. The site of origin and route and rate of migration of neurons to the hippocampal region of the rhesus monkey. J. Comp. Neurol. 196, 129–154.

Oliveras, J.L., Martin, G., Vos, B., Montagne, J., 1990. A single-unit recording system, contact thermal probe and electromechanical stimulator for studying cellular mechanisms related to nociception at brain stem level of awake, freely moving rats. J. Neurosci. Methods 35, 19–29.

Packard Jr., D.S., Menzies, R.A., Skalko, R.G., 1973. Incorporation of thymidine and its analogue, bromo-deoxyuridine, into embryos and maternal tissues of the mouse. Differentiation 1, 397–405.

Parent, J.M., Janumpalli, S., McNamara, J.O., Lowenstein, D.H., 1998. Increased dentate granule cell neurogenesis following amygdala kindling in the adult rat. Neurosci. Lett. 247, 9–12.

Parent, J.M., Tada, E., Fike, J.R., Lowenstein, D.H., 1999. Inhibition of dentate granule cell neurogenesis with brain irradiation does not prevent seizure-induced mossy fiber synaptic reorganization in the rat. J. Neurosci. 19, 4508–4519.

Parent, J.M., Yu, T.W., Leibowitz, R.T., Geschwind, D.H., Sloviter, R.S., Lowenstein, D.H., 1997. Dentate granule cell neurogenesis is increased by seizures and contributes to aberrant network reorganization in the adult rat hippocampus. J. Neurosci. 17, 3727–3737.

Paxinos, G., Watson, C., 1986. The Rat Brain in Stereotaxic Coordinates. Academic Press, Sydney.

Rakic, P., 1985. Limits of neurogenesis in primates. Science 227, 1054–1056.

Ratka, A., Sutano, W., Bloemers, M., de Kloet, E.R., 1989. On the role of brain mineralocorticoid (type I) and glucocorticoid (type II) receptors in neuroendocrine regulation. Neuroendocrinology 50, 117–123.

Reul, J.M., de Kloet, E.R., 1985. Two receptor systems for corticosterone in rat brain: microdistribution and differential occupation. Endocrinology 117, 2505–2512.

Ribak, C.E., Navetta, M.S., 1994. An immature mossy fiber innervation of hilar neurons may explain their resistance to kainate-induced cell death in 15-day-old rats. Dev. Brain Res. 79, 47–62.

Sankar, R., Shin, D., Liu, H., Katsumori, H., Wasterlain, C.G., 2000. Granule cell neurogenesis after status epilepticus in the immature rat brain. Epilepsia 6, S53–S56.

Sankar, R., Shin, D.H., Wasterlain, C.G., 1997. Serum neuron-specific enolase is a marker for neuronal damage following status epilepticus in the rat. Epilepsy Res. 2, 129–136.

Sapolsky, R.M., Krey, L.C., McEwen, B.S., 1985. Prolonged glucocorticoid exposure reduces hippocampal neuron number implications for aging. J. Neurosci. 5, 1222–1227.

Sapolsky, R.M., Meaney, M.J., 1986. Maturation of the adrenocortical stress response: neuroendocrine control mechanisms and the stress hyper-responsive period. Brain Res. 396, 64–76.

Sarkisian, M.R., Tandon, P., Liu, Z., Yang, Y., Hori, A., Holmes, G.L., Stafstrom, C.E., 1997. Multiple kainic acid seizures in the immature and adult brain: ictal manifestations and long-term effects on learning and memory. Epilepsia 38, 1157–1166.

Scharfman, H.E., Goodman, J.H., Sollas, A.L., 2000. Granule-like neurons at the hilar/CA3 border after status epilepticus and their synchrony with area CA3 pyramidal cells: functional implications of seizure-induced neurogenesis. J. Neurosci. 20, 6144–6158.

Schlessinger, A.R., Cowan, W.M., Gottlieb, D.I., 1975. An autoradiographic study of the time of origin and the pattern of granule cell migration in the dentate gyrus of the rat. J. Comp. Neurol. 159, 149–175.

Scott, B.W., Wang, S., Burnham, W.M., DeBoni, U., Wojtowicz, J.M., 1998. Kindling-induced neurogenesis in the dentate gyrus of the rat. Neurosci. Lett. 248, 73–76.

Scott, B.W., Woitowicz, J.M., Burnham, W.M., 2000. Neurogenesis in the dentate gyrus of the rat following electroconvulsive shock seizures. Exp. Neurol. 165, 231–236.

Seress, L., Ribak, C.E., 1990. Postnatal development of the light and electron microscopic features of basket cells in the hippocampal dentate gyrus of the rat. Anat. Embryol. 181, 547–565.

Sloviter, R.S., Sollas, A.L., Dean, E., Neubort, S., 1993. Adrenalectomy-induced granule cell degeneration in the rat hippocampal dentate gyrus: characterization of an in vivo model of controlled neuronal death. J. Comp. Neurol. 33, 324–336.

Sloviter, R.S., Valiquette, G.M., Abrams, E.C., Ronk, A.I., Sollas, L.A., Paul, S.L., Neubort, S.L., 1989. Selective loss of hippocampal granule cells in the mature rat brain after adrenalectomy. Science 243, 535–538.

Sperber, E.F., Haas, K.Z., Stanton, P.K., Moshé, S.L., 1991. Resistance of the immature hippocampus to seizure-induced synaptic reorganization. Dev. Brain Res. 60, 88–93.

Suga, S., Wasterlain, C.G., 1980. Effects of perinatal seizures or anoxia on cerebellar mitotic activity in the rat. Exp. Neurol. 67, 573–580.

Talmi, M., Carlier, E., Bengelloun, W., Soumireu-Mourat, B., 1995. Synergistic action of corticosterone on kainic acid-induced electrophysiological alterations in the hippocampus. Brain Res. 704, 97–102.

Tanapat, P., Gould, E., 1998. Adrenal steroids and N-methyl-D-aspartate receptor activation regulate neurogenesis in the dentate gyrus of adult rats through a common pathway. Neuroscience 82, 349–354.

van Pragg, H., Christie, B.R., Sejnowski, T.J., Gage, F.H., 1999. Running enhances neurogenesis, learning, and long-term potentiation in mice. Proc. Natl. Acad. Sci. USA 96, 13427–13431.

Vazquez, D.M., 1998. Stress and the developing limbic-hypothalamic-pituitary-adrenal axis. Psychoneuroendocrinology 23, 336–700.

Viau, V., Sharma, S., Meaney, M.J., 1996. Changes in plasma adrenocorticotropin, corticosterone, corticosteroid binding globulin, and hippocampal glucocorticoid receptor occupancy/translocation in rat pups in response to stress. J. Neuroendocrinol. 8, 1–8.

Wagner, J.P., Black, I.B., DiCicco-Bloom, E., 1999. Stimulation of perinatal and adult brain neurogenesis by subcutaneous injection of basic fibroblast growth factor. J. Neurosci. 19, 6006–6016.

Wasterlain, C.G., 1976. Effects of perinatal status epilepticus on rat brain development. Neurology 26, 975–986.

Wasterlain, C.G., 1979. Does anoxemia play a role in the effects of perinatal seizures on brain growth? An experimental study in the rat. Eur. Neurol. 18, 222–229.

Wasterlain, C.G., Plum, F., 1973. Vulnerability of developing rat brain to electroconvulsive seizures. Arch. Neurol. 29, 38–45.

Young, E.A., Spencer, R.L., McEwen, B.S., 1990. Changes at multiple levels of the hypothalamo-pituitary adrenal axis following repeated electrically induced seizures. Psychoendocrinology 15, 165–172.